Julien, M., Zhao, Y., Ma, R., Zhou, Y., Nakagawa, M., Yamada, K., Yoshida, N., Remaud, G. S., Gilbert, A. (2022): Re-evaluation of the 13C isotope fractionation associated with lipids biosynthesis by position-specific isotope analysis of plant fatty acids. - Organic Geochemistry, 174, 104516.

https://doi.org/10.1016/j.orggeochem.2022.104516

Re-evaluation of the ^{13}C isotope fractionation associated with lipids biosynthesis by position-specific isotope analysis of plant fatty acids

Maxime Julien[a,b]*, Yu Zhao[c], Ran Ma[c], Youping Zhou[c,d], Mayuko Nakagawa[b,e], Keita Yamada[f], Naohiro Yoshida[f,g], Gérald S. Remaud[h], Alexis Gilbert[b,e]

a. GFZ German Research Centre for Geosciences - Helmholtz Centre Potsdam, Organic Geochemistry, Potsdam, Germany.

b. Department of Earth and Planetary Sciences, Tokyo Institute of Technology, Meguro, 152-8551 Tokyo, Japan.

c. Isotopomics in Chemical Biology (ICB), School of Chemistry & Chemical Engineering. Shaanxi University of Science and Technology, Xi'an, China.

d. Department of Ocean Science and Engineering, Southern University of Science and Technology (SUSTech), Shenzhen, 518055, China.

e. Earth-Life Science Institute, Tokyo Institute of Technology, Meguro, 152-8550 Tokyo, Japan.

f. Department of Environmental Chemistry and Engineering, Tokyo Institute of Technology, Yokohama, 226-8503 Kanagawa, Japan.

g. National Institute of Information and Communications Technology, Koganei, 184-8795 Tokyo, Japan.

h. CNRS, CEISAM UMR 6230, Nantes Université, 2 rue de la Houssinière, BP 92208, 44000 Nantes, France.

mail: mjulien@gfz-potsdam.de

Abstract

Carbon-13 position-specific isotope analysis of fatty acids from vegetable oils is performed using Nuclear Magnetic Resonance in the present study. The measured ^{13}C patterns are not totally in accordance with the conventional view of the relative ^{13}C-depletion of acetogenic lipids and their alternation of ^{13}C-enriched and ^{13}C-depleted carbon positions. The results presented here provide a new evaluation of the isotopic fractionation associated with fatty acids biosynthesis. Whereas it is commonly admitted that the pyruvate dehydrogenase (PDH) is responsible for the ^{13}C distribution within fatty acids, data from the present work demonstrate that the conversion of acetyl-CoA to malonyl-CoA catalyzed by acetyl-CoA carboxylase (ACC) needs to be considered while explaining the measured non-stochastic ^{13}C pattern within fatty acids. These data combined with steady-state calculation give a new description of metabolic steps responsible for the acetogenic lipids typical ^{13}C intramolecular distribution. In addition, the non-stochastic pattern measured in these plant fatty acids is similar to previously detected within long-chain *n*-alkanes suggesting a preservation through geological time and demonstrating the interest of position-specific isotope analysis for studying the evolution of metabolic pathways.

Keywords

fatty acids biosynthesis – carbon isotopes – isotopomers – isotope fractionation – NMR

1. Introduction

Stable isotope of light elements (C, H, O, N, S) are employed to trace biogeochemical cycles in present and past Earth environments. The isotopic composition of biomolecules is directly linked to their source, the pathway and fluxes associated with their biosynthesis and external factors such as temperature or the CO_2 pressure. Thus, the isotopic composition records the conditions of their biosynthesis. Lipids are an important class of biomarkers as they are preserved in sediments under different chemical forms, (free lipids, bitumen, kerogen), and their isotope compositions can be an important source of information.

The determination of lipids isotopic composition $\delta^{13}C$ have flourished in the 1990's with the development of compound-specific isotope analysis (CSIA) which allows the determination of $\delta^{13}C$ values of several compounds in the same run coupling isotope ratio mass spectrometry (IRMS) with gas chromatography (GC). The advantage of CSIA is an increased amount of information compared with bulk approaches which give a weighted average of all molecules within the sample. Hence, the discrimination potential can be greatly enhanced (Hayes, 1993). In addition, when analytes have a specific chemical structure characteristic of the production by a metabolic pathway from organisms ("biomarkers"), their isotope compositions provide a way to assess their source (Valentine, 2009) and to identify precursors for lipid biosynthesis (Zhou et al., 2010).

Thus far, most $\delta^{13}C$ measurements of organic molecules are made after their conversion to CO_2 which allows the precision required to observe natural abundance variations. The conversion step leads to a $\delta^{13}C$ value which is the average of $\delta^{13}C$ values from all positions in the molecule. The measurement of δ values of given positions within a molecule, called position-specific isotope analysis (PSIA), is only accessible via specific methods (Gilbert, 2021): chemical or enzymatic degradation of specific C-atom positions and subsequent $\delta^{13}C$ determination (Monson and Hayes, 1980; Rossmann et al., 1991), in-source fragmentation in a

mass spectrometer (Eiler et al., 2013; Neubauer et al., 2018), thermal breakdown coupled to IRMS analysis ("on-line pyrolysis") (Corso and Brenna, 1997; Gilbert et al., 2016) and direct analysis by nuclear magnetic resonance (Jézéquel et al., 2017; Akoka and Remaud, 2020).

While the amount of position-specific δ values on natural molecules is scarce, data collected so far report that (i) most, if not all, organic molecules follow a non-stochastic pattern, i.e., the δ values for different positions in the same molecule is not equal and (ii) these values can bring new constraints on the origin and history of a given molecule. Important applications include food authentication (with the measurement of molecules such as ethanol, acetic acid, caffeine, vanillin), tracing the fate of hydrocarbons and other pollutants (Gilbert et al., 2009; Yamada et al., 2014; Diomande et al., 2015; Julien et al., 2016; Portaluri et al., 2021) and recently cosmochemistry (Chimiak et al., 2021). All these studies take advantage of natural isotope fractionation associated with the (bio)synthesis of organic molecules which, because it involves breaking and forming specific C-C bonds, leads to heterogeneous isotope distributions. Hence, PSIA can potentially inform on the biological pathway and physiological status of a given organism. Applied to geochemistry, this could be an invaluable tool to trace metabolic pathways and physiological status in present and past ecosystems.

In that context, lipids represent target molecules of huge interest. While lipid ^{13}C-CSIA are commonly used to trace short-term and long-tern biogeochemical changes (Schouten et al., 1998), PSIA of lipids has been limited to a number of studies on fatty acids (Monson and Hayes, 1980, 1982a, 1982b) and alkanes (Gilbert et al., 2013). At the molecular level, fatty acids are systematically depleted in ^{13}C in comparison to other compounds such as sugars or amino acids (Hayes, 2001), with the notable exception of those synthesized by organisms using the reductive tricarboxylic acid (rTCA) pathway (van der Meer et al., 1998). DeNiro and Epstein showed that the ^{13}C-depletion in lipids was due to the normal isotopic effect ($^{12}k/^{13}k > 1$) associated with the oxidative decarboxylation of pyruvate into acetyl-CoA catalyzed by pyruvate

dehydrogenase (PDH) (DeNiro and Epstein, 1977). Acetyl-CoA formed from pyruvate is thus ^{13}C-depleted, and so are the lipids formed therefrom. Notably, the isotope effects associated with the pyruvate oxidative decarboxylation are position-specific, the depletion in acetyl-CoA formed being located in the carbonyl position, the methyl position being hardly affected (Fig. 1). Two observations follow: acetyl-CoA has a heterogeneous pattern which is transferred to fatty acids through the fatty acid synthase, leading to a "zig-zag" pattern throughout the carbon chain: odd positions must be ^{13}C-depleted compared with even positions; (ii) the extent of the depletion depends on the isotope effect of the enzyme and on the commitment of the PDH reaction: it is maximum at low commitment values and becomes null when the decarboxylation of pyruvate is 100%.

Through chemical degradation, Monson and Hayes (1980) measured the carboxyl and unsaturated C-atom positions of unsaturated fatty acids from *Escherichia coli* (*E. coli*) grown with glucose as the sole carbon source. Their results are in accordance with the hypothesis made by DeNiro and Epstein (1977) with a depletion of 6‰ on odd positions. The commitment of pyruvate decarboxylation in *E. coli* was measured to be 0.75 (Roberts et al., 1955), thus a 6‰ depletion corresponds to a KIE of 1.023. The latter value was later confirmed by the *in vitro* determination using the isolated enzyme purified from *E. coli* (1.021; (Melzer and Schmidt, 1987)). These pioneering studies allowed the elucidation of the origin of the ^{13}C-depletion in lipids, and also showed the importance of PSIA to understand the bulk isotope composition of biosynthesized organic molecules. The calculation derived from the data Monson and Hayes (1980) is based on the assumption that the isotope pattern of the starting glucose fed to *E. coli* is homogeneous (Hayes, 2001). Later studies have proven this to be wrong (Rossmann et al., 1991; Gilbert et al., 2009; Gilbert et al., 2012). Although, using the latest data on corn glucose (the same type of glucose as used by Monson and Hayes) measured by NMR, and the most recent commitment value of 0.83 (Chen et al., 2011), gives a value of 1.025, still very similar to the experimental value determined by Melzer and Schmidt (1987).

Yet, several issues are still challenging the simple explanation given above. First, the data obtained on fatty acids are scarce and limited to specific position within the molecule. The method used to collect these data involved the chemical degradation of fatty acids followed by the isotope analysis of the generated fragments. The data available are thus those for positions prone to chemical degradation, namely carboxyl and unsaturated positions of the fatty acids. From a metabolic viewpoint, these positions are involved in reactions occurring besides acetyl-CoA polymerization, namely, transesterification and reduction, respectively. The interpretation of the data thus requires careful consideration of these additional steps that are potentially prone to isotope fractionation. The measurement of saturated positions (CH_2 and CH_3), which isotope fractionation is not altered be secondary biochemical reactions, would therefore be beneficial to understand the determinants governing the isotope composition of biological lipids.

Second, the current paradigm considers the isotopic fractionation associated with PDH catalyzed reaction as the only determinant of the ^{13}C distribution within acetyl-CoA. However, several other reactions involved in acetyl-CoA formation and degradation are potentially associated with isotope fractionation and must thus be considered. For instance, acetyl-CoA in *E. coli* is not solely used for fatty acid biosynthesis and can be used for the synthesis of several other metabolites (citrate, acetate) which isotope effects are unknown but likely not negligible. Notably, acetate excreted from *E. coli* has been shown to be 24‰ enriched on the carboxyl position, the methyl position being unfractionated compared to the starting glucose (Blair et al., 1985). Recent studies have shown that acetate can be re-assimilated through the phosphate acetyltransferase and acetate kinase (Pta-AckA) pathway through the formation of acetyl-phosphate (Enjalbert et al., 2017). Given the bidirectionality of the acetate/acetyl-P/acetyl-CoA reactions, the isotope pattern of acetate will likely influence that of acetyl-CoA. Other reactions linked to acetyl-CoA may also be prone to isotope fractionation. In particular the first step of the Krebs cycle catalyzed by citrate synthase is thought to be associated with an isotope effect of 1.023 (Tcherkez and Farquhar, 2005). These reactions should be considered when

148 interpreting the ^{13}C isotope pattern in acetogenic lipids. Second, the data from fatty acids
149 extracted from *Saccharomyces cerevisiae* (*S. cerevisiae*) using the same glucose as the carbon
150 source showed a reverse pattern, i.e., with odd and even positions enriched and depleted,
151 respectively, compared to the starting glucose. This observation has found no clear account yet.
152 Finally, the chemical degradation method used by Monson and Hayes (1980; 1982) implies that
153 the positions analyzed are labile C-atoms positions, i.e., the carboxyl and the unsaturated C-
154 atom positions. These are involved in several biosynthetic reactions in the cell once fatty acids
155 are formed (hydrolysis/esterification and dehydrogenation, respectively) which isotope
156 fractionation can alter the signature of the original C-atoms. Clearly therefore, gaining a
157 comprehensive view on the isotope fractionation associated with lipid biosynthesis requires a
158 re-examination of natural intramolecular isotope composition of fatty acids.

159 In this study, we use isotopic ^{13}C NMR to measure the position-specific isotope
160 composition of fatty acids from coconut and sunflower oils. NMR is currently the only approach
161 capable of determining the ^{13}C position-specific isotopic composition of fatty acids, including
162 their CH_2 and CH_3 (see Supplementary Fig. S3). The choice of using vegetable oils is obvious
163 when considering the amount necessary for isotopic NMR measurements, namely, few hundred
164 milligrams of pure compound. In addition, the advantage of studying fatty acids biosynthesis is
165 that the commitment of acetyl-CoA to lipids is around 100% in plant seeds (Schwender et al.,
166 2006; Alonso et al., 2007; Alonso et al., 2010), making it a very simple system. Isotopic ^{13}C
167 NMR allows the measurement of 6 C-atom spectral resolved positions within the carbon chain
168 of fatty acids. Carbon-13 NMR spectra present a large chemical shift range theoretically
169 allowing the $\delta^{13}C$ measurement of many C-positions. However, CH_2 located in long carbon
170 chains all have similar electronic environments leading to peak overlap. In this context, PSIA
171 of FAMEs by ^{13}C NMR only allows measuring 6 carbon positions when the carbon chain is >
172 C_{10}. In addition, we use a chemical method previously used for ^{2}H measurements (Billault et
173 al., 2001) to break the double bond of unsaturated fatty acids and have access to 12 C-atoms,

providing further insights into the origin of the isotope fractionation in fatty acids. We then discuss the potential metabolic steps responsible for the pattern observed in the context of metabolic fluxes and potential enzymatic isotope effects. This study thus represents an additional step towards understanding the isotope fractionation associated with lipids biosynthesis.

2. Materials and Methods

2.1. Chemicals

Coconut oil, methyl palmitate standard (C16:0), methanol, boron trifluoride 10% in methanol (BF_3/methanol), dichloromethane, magnesium sulfate ($MgSO_4$), sodium chloride (NaCl), silica gel (70–230 mesh), silver nitrate ($AgNO_3$), *n*-hexane, cyclohexane, ethyl acetate, acetone, OsO_4 (2.5% in *tert*-butanol), NMO (*N*-methylmorpholine oxide), $Na_2S_2O_3$, $NaIO_4$, were purchased from Sigma Aldrich (Sigma-Aldrich, MO, USA). Methyl oleate (C18:1) from sunflower was obtained from Sigma Aldrich and was certified from sunflower oil (Product: 311111 Lot:040M3401). Toluene-d_8 was purchased from Wako Pure Chemical Industries, Ltd. (Osaka, Japan). The relaxing agent (tris(2,4-pentadionato)chromium(III) [$Cr(Acac)_3$]) was purchased from Kanto Chemical Co., Inc. (Tokyo, Japan).

2.2. Fatty acid methyl esters preparation from vegetable oils

Transesterification of vegetable oil was directly performed in a 250 mL round bottom flask (Morrison and Smith, 1964). Forty mL of methanol were mixed with 1 g of oil and the mixture was boiled for 10 min under reflux. Then, 20 mL of boron trifluoride 10% in methanol was slowly introduced and the boiling was kept for 5 more minutes before the addition of 20 mL of dichloromethane and an additional minute under reflux. After cooling, the mixture was transferred into a separating funnel in which 30 mL of dichloromethane and 30 mL of saturated NaCl solution were added. The organic phase, containing the FAMEs, was washed with 20 mL

deionized water, isolated again, dried using $MgSO_4$ and filtered. The solvent was evaporated using a rotary evaporator. This process is then repeated in order to accumulate enough FAMEs extracts.

2.3. Isolation of saturated FAMEs

The separation of saturated and unsaturated FAMEs was performed by modified argentation column chromatography on silica gel (Duan et al., 2002). The silver-doped silica gel was prepared mixing 110 g silica gel with 80 mL solution of silver nitrate 50% in deionized water. The mixture was dried at 120 °C for 24 h. The flash chromatography column was packed mixing the silver-doped silica gel with 100 mL of cyclohexane. After sample deposit (maximum 2 g of FAMEs mixture), the elution was performed as followed: 1 L cyclohexane, 2 L cyclohexane/AcOEt (99.5:0.5, v/v), 1 L cyclohexane/AcOEt (99:1, v/v). Fractions of 20 mL were collected and the presence of FAMEs was checked by gas chromatography.

2.4. Separation of saturated FAMEs

The separation of single saturated FAMEs was performed by preparative Liquid Chromatography purchased from Shimadzu (Kyoto, Japan) equipped with a UV detector operating at 254 nm. Two preparative reversed-phase columns were used in parallel: a 5C18-PAQ (20 × 250 mm) purchased from Cosmosil (Kyoto, Japan) and a 5μm C8 (20 × 250 mm) purchased from Shimadzu (Kyoto, Japan). Both columns were maintained at 40 °C for higher stability of retention times. One mL sample was injected (maximum 500 mg of saturated FAMEs in hexane, collected from the previous step 2.3.) and the elution was performed using methanol/water (90:10, v/v). Single saturated FAMEs were collected and the purification was repeated until obtaining the required amount for both bulk and position-specific ^{13}C isotope analyses. Only the most abundant saturated FAMEs were collected for further analysis (C12:0, C14:0 and C16:0 in the case of coconut oil sample).

222 *2.5. Chemical modification of methyl oleate from sunflower*

223 Methyl oleate (compound A in Fig. 2) was converted into nonanol and methyl 9-
224 hydroxynonanonate (compounds C and D in Fig. 2 respectively) as followed (Volchkov et al.,
225 2011). First, 60mL of methyl oleate in an acetone/water (5:1, v/v) solution at 0.08 M. To this
226 mixture, 146 mg of OsO_4 (2.5% in *tert*-butanol) and 1.37 g of NMO were added at room
227 temperature and stirred for 6 h. After removing acetone using rotary evaporator, 10 mL of
228 saturated $Na_2S_2O_3$ solution were added to the residue and stirred for 20 min. The mixture was
229 transferred into a separating funnel and extracted with 40 mL ethyl acetate three times. The
230 combined organic phase was dried using Na_2SO_4, filtered and concentrated under vacuum. The
231 residue was purified by flash column chromatography, using *n*-hexane/ethyl acetate (4:1, v/v)
232 as eluent, to obtain methyl 9,10-dihydroxyoleate (compound B in Fig. 2, yield = 96%). The
233 compound B was resuspended into 12 mL of methanol/water (4:1, v/v) and 159 mg of $NaIO_4$
234 were added at 0 °C. The reaction mixture was stirred for 4 h under N_2 protection at room
235 temperature. Then, 136 mg $NaBH_4$ were added to the mixture solution and stirred 40 min at 0
236 °C. After this reaction, 10 mL water were added at 0°C and the mixture was extracted three
237 times with 30 mL ethyl acetate. The combined organic phase was washed with saturated
238 aqueous NaCl solution, dried using Na_2SO_4, and concentrated under vacuum. The residue was
239 purified by flash silica column chromatography, using a gradient of cyclohexane/ethyl acetate
240 (from 20:1 to 6:1, v/v), to obtain nonanol (compound C in Fig. 2, yield = 85%) and methyl 9-
241 hydroxynonanonate (compound D in Fig. 2, yield = 80%).

242 *2.6. ^{13}C compound specific isotope analysis*

243 The ^{13}C isotopic composition of each FAME was measured using a gas chromatograph
244 coupled with the isotope ratio mass spectrometer (DeltaPlusXP, Thermo Fisher Scientific) via
245 a combustion furnace and an open split interface (GC Combustion III, Thermo Fisher
246 Scientific). High purity helium (> 99.99%) was used as a carrier gas. Samples were diluted in

hexane before injection in the GC equipped with a capillary column (DB-5, 30 m × 0.32 mm i.d., 0.25 µm film thickness; Agilent J&W) using a 10 µL syringe and the employed separation conditions were as followed: injector temperature 250 °C; split ratio 10:1; flow rate at 1.5 mL/min; initial oven temperature was 50 °C maintained during 5 min then raised to 250 °C (10 °C/min) and maintained during 10 min. After leaving the GC, the effluent entered a combustion furnace (operating at 960 °C) containing a ceramic tube packed with CuO, NiO and Pt wires. The generated CO_2 was then analyzed in the IRMS. In order to check GC-C-IRMS accuracy, the methyl oleate standard from sunflower was also analyzed by off-line combustion, CO_2 purification followed by IRMS measurement. No significant $\delta^{13}C$ difference was detected between the two methods so no further data correction was required. The $\delta^{13}C$ data for individual FAMEs are presented in Table 1.

2.7. ^{13}C position-specific isotope analysis

The ^{13}C distribution within FAMEs was determined by isotope ratio monitoring by ^{13}C NMR. PSIA by ^{13}C-NMR is now well documented (see for example a recent review Akoka and Remaud 2021), although, for readers not familiar with the technique further details are given in SI. Sample preparation consisted in the successive addition in a 4 mL vial the studied fatty acid methyl ester, nonanol or 9-hydroxynonanonate and toluene-d_8, as lock signal-containing the relaxing agent. The volume of toluene-d_8 and the concentration of CrAcac were adapted depending on the carbon chain length, the quantity available and according to the T_1 values (longitudinal relaxation). All samples were analyzed using the same sample preparation: 100 mg of pure sample mixed with 600 µL of toluene-d_8 containing 25 mM of relaxing agent [$Cr(Acac)_3$]. The volume of solvent containing $Cr(Acac)_3$ was adapted to the amount of sample available after purification to always use the same sample concentration and sample/relaxing agent ratio. The interaction between the analyte (fatty acid methyl ester here) and the relaxing agent diminishes the T_1 leading to shorter measurements. However, T_1 values should not be

shorter than the acquisition time (AQ) to avoid any Nuclear Overhauser Effect (NOE). Therefore, the concentrations of FAME and relaxing agent need to be adapted according to the amount of analyte available (see Supplementary information "Details on PSIA by ^{13}C NMR approach" for further explanation). Then, the sample was introduced into a 5 mm NMR tube.

Quantitative ^{13}C NMR spectra were recorded using a Bruker 400 Avance III spectrometer fitted with a 5 mm o.d. $^{13}C/^{1}H$ probe carefully tuned at the recording frequency of 100.64 MHz. The temperature was set at 303 ± 0.1 K, without tube rotation. The offset for both ^{13}C and ^{1}H was set at the middle of the frequency range observed for each compound studied. An inverse-gated decoupling technique was used to avoid any Nuclear Overhauser Effect (NOE). A cosine adiabatic pulse with appropriate phase cycles was employed as proton decoupling sequence (Tenailleau and Akoka, 2007). A repetition time/inter-pulse delay, greater than ten times the longest T_1 of each compound was used and the acquisition parameters were adjusted to obtain a signal-to-noise ratio (S/N) > 700. From previous experiments, S/N > 700 usually leads to a standard deviation for precision of around 0.7‰ (Caytan et al., 2007; Botosoa et al., 2008; Thomas et al., 2010; Gilbert et al., 2011; Bayle et al., 2014, 2015; Julien et al., 2021). Five spectra were recorded for each measurement: the values for each studied carbon position are the mean of the five spectra. Free induction decay was submitted to an exponential multiplication inducing a line broadening of 2 Hz. The curve fitting was based on a total-line-shape analyses (deconvolution) carried out with a Lorentzian mathematical model using Perch Software (PerchTM NMR Software, http://www.perchsolutions.com).

Since the signals corresponding to the central CH_2 atoms overlap in the 28–30 ppm region for fatty acids longer than C_{10} at the magnetic field used (400 MHz spectrometer), only the isotopomers bearing a ^{13}C atom in one of the three terminal positions of the carboxylic acid side (COOH, $CH_{2\alpha}$, $CH_{2\beta}$) or of the aliphatic chain side (CH_3, CH_{2a} and CH_{2b}) could be quantified (see Fig. 3 for further details). PSIA of both nonanol (compound C) and 9-

hydroxynonanoate (compound D) present the same limitation leading to the measurement of 6 carbon positions within each of them (see Fig. 3). The carbon bearing the alcohol function (COH) and its two neighbors ($CH_{2\alpha}$, $CH_{2\beta}$) within both compounds C and D, the three terminal positions of the aliphatic chain side (CH_3, CH_{2a} and CH_{2b}) of compound C and the carbon bearing the methyl ester function of compound D (COOMe and its two neighbors CH_{2a} and CH_{2b}) could be measured using isotopic ^{13}C NMR. For each of these carbon atom positions, the relative ^{13}C abundance was determined using the molar fraction f_i (where i is the C atom position considered) as follows: $f_i = S_i/S_{tot}$, where S_i is the area of the peak corresponding to the ^{13}C isotopomer in the position i and S_{tot} the total area of the peaks corresponding to the six ^{13}C isotopomers ($S_{tot} = S_{COOH/COH} + S_{CH2\alpha} + S_{CH2\beta} + S_{CH3/COOMe} + S_{CH2a} + S_{CH2b}$). Each S_i was corrected to compensate for the slight loss of intensity caused by satellites (interactions due to the presence of ^{13}C–^{13}C isotopologues) by multiplying by $(1 + n \times 0.011)$, where n is the number of carbons directly attached to the C atom position i (n = 1 for the COOH, COH, COOMe and CH_3 positions and n = 2 for the $CH_{2\alpha}$, $CH_{2\beta}$, CH_{2a} and CH_{2b} positions) and 1.1% (= 0.011) is the average natural ^{13}C abundance (Tenailleau et al., 2005; Silvestre et al., 2009). Eventually, if F_i denotes the statistical mole fraction (homogeneous ^{13}C distribution, i.e. $F_i = 1/6$ for each carbon position in the case of FAMEs, nonanol and 9-hydroxynonanoate) at any C atom position i, then the position-specific relative deviation from a ^{13}C homogeneous distribution is $\Delta\delta^{13}C$ (‰) = $(f_i/F_i - 1) \times 1000$. When $\Delta\delta^{13}C > 0$ the C-position i is relatively enriched and relatively impoverished when $\Delta\delta^{13}C < 0$ (see Fig. 3–6). In Fig. 4, carboxyl position is not taken into account in the determination of ^{13}C distribution, so the same calculation applies but taking into account only the 5 other positions and F_i becomes 1/5.

Importantly, different NMR probe configuration can introduce systematic errors in the isotopic measurement (Jézéquel et al., 2017). For some probe configurations, shielded positions (typically COO positions) appear ^{13}C-richer and deshielded positions (typically, CH_3) appear

322 ^{13}C-poorer (Bayle et al. 2015). In order to ensure trueness of the measurements, a correction
323 was made by measuring a methyl palmitate standard on both the NMR spectrometer of
324 CEISAM laboratory (Nantes Université) which has been shown to provide δ^{13}C values, close
325 to the "true values" as found for acetic acid (Bayle et al., 2015), and values from the
326 spectrometer used in this study (in Tokyo Institute of Technology, Japan). Corrections of –8‰
327 and +3‰ were applied to COOH and CH_3 positions, respectively. This correction was applied
328 to all fatty acid methyl esters, as well as to the methyl 9-hydroxynonanonate.

329 In addition, future investigations could be extended to the study of chiral fatty acids
330 using ^{13}C NMR in presence of chiral liquid crystals (CLCs). This recently developed method
331 allows the separation of the enantiomers in NMR spectrum leading to the measurement of the
332 intramolecular ^{13}C distribution within the different enantiomers. Using this technique, the ^{13}C
333 enantiofractionations associated with the biosynthesis of chiral fatty acids could be revealed
334 (Lesot et al., 2021).

335 **3. Results and discussion**

336 *3.1 Variability on the carboxyl position*

337 The results of the $\Delta\delta^{13}$C values are reported in Fig. 3. Standard deviations from the mean
338 for 3–5 measurements are below 1‰, which is consistent with previous measurements at the
339 same signal/noise ratio. $\Delta\delta^{13}$C values range from –16.3‰ to 20.6‰, with the C-1 position
340 exhibiting the most variable values. The transesterification of triglycerides to fatty acid methyl
341 esters could be invoked to explain the variability as it involves breaking and forming C-O bonds
342 and it is thus conceivable to expect the presence of an isotope effect. However this reaction is
343 considered quantitative (Duron and Nowotny, 1963; Metcalfe et al., 1966) and is commonly
344 used for transesterification of vegetable oils prior to their qualitative and quantitative analysis
345 (Chapman, 1979; Chawla, 2003). In addition, FAMEs from coconut oil were all transesterified
346 in the same conditions, but show the highest variability in our dataset, with both strong ^{13}C-

enrichments and depletions (Fig. 3). Hence, while we do not exclude isotope effects occurring during the transesterification reaction, these cannot explain the observed variation on the carboxyl position. Rather, we propose that the variability on C-1 position arises from metabolic isotope fractionation during the synthesis and degradation of triglycerides. After fatty acids are produced, the C-1 (carboxyl) position is involved in several esterification reactions with a molecule of glycerol to produce di- or triglycerides which are the main constituent of vegetable oils. The presence of isotope fractionation during this biosynthesis step and the variable concentration of the different fatty acids could explain the high variability of $\delta^{13}C_{C\text{-}1}$. Our data are indeed consistent with that of Vogler and Hayes (1980) who showed that the $\delta^{13}C$ value of the carboxyl positions of fatty acids extracted from soybean, nutmeg and corn exhibited high variability, with $\Delta\delta^{13}C_{Carboxyl}$ values (= $\delta^{13}C_{Carboxyl} - \delta^{13}C_{FA}$) ranging from –9.9‰ to +8.8‰ (Vogler and Hayes, 1979). They conclude that "none of the carboxyl-group compositions can safely be taken as representative of the carbonyl group in the acetyl-CoA inter- mediate" (Vogler and Hayes, 1979). Our data corroborates their conclusion and the $\Delta\delta^{13}C$ of C-1 will not be discussed further here. Data presented in this study clearly demonstrate that carboxyl position of fatty acids should not be considered while studying the ^{13}C intramolecular distribution within fatty acids. Moreover, a difference of around 12‰ is observed between the $\delta^{13}C_{C\text{-}1}$ of sunflower sample before and after the cleavage. This alteration might be explained by isotope fractionation associated with the esterification, the cleavage and/or the purification of compounds C and D, while the reaction/purification yield is ≥ 80% (Fig. 2).

The data NMR provides are relative to the sum of all isotopomers. Therefore, the high variability on the C-1 position can affect the $\Delta\delta^{13}C$ value of all other positions. We thus built Fig. 4 without considering the C-1 positions (calculation of S_{tot} without using S_{COOH}, see part *2.7*). Fig. 4 shows a saw-toothed pattern with odd positions systematically ^{13}C-enriched compared to their adjacent even positions, and *vice versa*. This is yet more apparent in Fig. 5

where the difference of $\Delta\delta^{13}C$ content between two adjacent positions ($\Delta\delta^{13}C_n = \delta^{13}C_n - \delta^{13}C_{n-1}$) are plotted against the carbon number. On average, the difference between even and adjacent odd positions ranges from –7.2‰ to –11.7‰ and that from odd and adjacent even positions range from +11.9‰ to +12.2‰ (Table 1). The only exception is the difference in $\Delta\delta^{13}C$ values between the subterminal (CH_{2a}) and terminal (CH_3) positions which average at 0.0‰ (Table 1). Qualitatively, the results of FAMEs from vegetable oil are comparable to those obtained from the yeast *S. cerevisiae* ($\delta^{13}C_{even}$-$\delta^{13}C_{odd}$ = –6.5‰) (Monson and Hayes, 1982b) and reverse that found in the bacterium *E. coli* ($\delta^{13}C_{even}$-$\delta^{13}C_{odd}$ = +6‰) (Monson and Hayes, 1980), see Fig. 6. Interestingly, carbon positions 9 and 10 of C18:1 from sunflower (measured after cleavage of the double bond, Fig. 2) have a similar ^{13}C relative depletion (Fig. 4). The absence of isotopic difference between these adjacent carbon-positions may be due to the presence of isotopic fractionation associated with the synthesis and purification of compounds C and D (Fig. 2), although the yield of the cleavage and isolation of these compounds is ≥ 80%. However, even if measured data are altered by a potential isotope fractionation, C-9 and C-10 do not follow the "zig-zag" pattern observed in other positions, which could be due to the absence of double bond reduction during this elongation step (see Fig. 7).

3.2 Impact of the ^{13}C intramolecular pattern of sugars

The data obtained here and in previous studies must be interpreted considering the position-specific ^{13}C isotope pattern of sugars, precursors of pyruvate and acetyl-CoA. Rossmann et al (1991) were the first to determine the $\delta^{13}C$ values for each of the 6 positions of glucose. They notably showed that the C-4 and C-6 positions were ^{13}C-enriched and ^{13}C-depleted respectively. Later, Gilbert et al. (2009) confirmed the pattern using ^{13}C NMR, and measured isotope effects associated with sugars interconversions, namely, sucrose hydrolysis by invertase and glucose isomerization to fructose by glucose isomerase (Gilbert et al., 2012). In plants plastid, pyruvate is fully committed to the formation of acetyl-CoA, therefore no

isotope fractionation is expected to occur during the PDH reaction as the conversion of pyruvate to acetyl-CoA is close to 100% (Schwender et al., 2006; Alonso et al., 2007; Alonso et al., 2010). Assuming a negligible isotope fractionation in the glycolytic process and pyruvate decarboxylation, the isotope composition of the methyl and carbonyl position of acetyl-CoA must be the average of C-1 and C-6 and that of C-2 and C-5 positions, respectively. Considering a C_3 sucrose (Gilbert et al., 2012) the relative enrichment on the methyl and carbonyl positions must be –3.7‰ and –0.2‰, respectively, leading to a difference of 3.5‰ between odd and even adjacent positions (see Table S1 in the Supporting Information). In fact, the substrate for pyruvate biosynthesis is fructose-6-phosphate. The conversion of glucose-6-P to fructose-6-P is associated with an equilibrium isotope effect which leads to a ^{13}C-enrichment on the C-2 position and a ^{13}C-depletion on the C-1 position of fructose, hence different patterns for glucosyl and fructosyl moieties of sucrose (Gilbert et al., 2012). Because it involves the C-1 and C-2 positions of fructose, glucose-fructose isomerization must thus play a role in shaping the ^{13}C-pattern of acetyl-CoA, to an extent depending on the fate of glucose vs fructose and potential isotope effects associated. Considering the fructosyl moiety of sucrose as the substrate for acetyl-CoA synthesis (the glucosyl moiety being used in the pentose-phosphate and starch synthesis (Alonso et al., 2007)), the relative ^{13}C composition of acetyl-CoA becomes –5.0‰ and +1.8‰ for methyl and carbonyl positions, respectively, leading to a difference of –6.8‰ between two adjacent positions (Fig. 6). This value qualitatively agrees with our data, although the difference between two adjacent positions in oils FAMEs is slightly higher (Table 1), for reasons that will become apparent below.

3.3 Role of the acetyl-CoA carboxylase

A striking feature when considering Fig. 5 and Table 1 is the relative ^{13}C-enrichment of the methyl positions compared with other even C-atom positions. Indeed, the difference between the subterminal (CH_{2a}) and the terminal (CH_3) positions is negligible (average 0.0 ±

422 3.8‰). Furthermore, the terminal CH_3 position is systematically ^{13}C-enriched compared to the
423 next even position (C_{n-2}; Fig. 5). This is in contradiction with the view that the pattern of acetyl-
424 CoA is fully transferred to the alkyl chain of fatty acids without isotope fractionation. Rather,
425 it suggests that there is a fractionating step between acetyl-CoA and fatty acids which enriches
426 the CH_3 position and/or depletes every other even position. Among the reactions involving the
427 CH_3 of acetyl-CoA, its carboxylation catalyzed by acetyl-CoA carboxylase (ACC) seems
428 plausible (Chan and Vogel, 2010). The reaction adds a carbonate to the CH_3 position of acetyl-
429 CoA, leading to the formation of malonyl-CoA (Fig. 7). Because a C-C bond is formed during
430 that step, an isotope fractionation on the CH_3 position of acetyl is conceivable. The CH_3 position
431 of acetyl-CoA must be ^{13}C-enriched, and the CH_2 position of malonyl-CoA must be ^{13}C-
432 depleted. Malonyl-CoA is then used as the C_2 elongation unit, and all even C-atom positions
433 will be ^{13}C-depleted compared with the acetyl-CoA. As a result, the terminal (CH_3) position of
434 fatty acids arising from acetyl-CoA and are ^{13}C-enriched, while the other even positions arising
435 from malonyl-CoA and are depleted. Qualitatively, this agrees with the observation made here
436 (see Fig. 3–5). The extent of the enrichment and depletion depends on the KIE and the
437 commitment of the reaction. The synthesis of a C_{16} chain requires the synthesis of 7 moles of
438 malonyl-CoA per mole of acetyl-CoA. At the steady-state, the flux of acetyl-CoA to malonyl-
439 CoA must be 7 times that of that to the synthesis of β-ketoacyl-ACP, leading to a relative
440 commitment of 7/8 = 0.875 to the formation of malonyl-CoA as described in Fig. 7. The
441 difference between the subterminal (CH_{2a}) and the terminal (CH_3) positions being 0.0‰ on
442 average, and assuming the original $\Delta\delta^{13}C$ between the methyl and carboxyl position of acetyl-
443 CoA is –6.8‰, then the kinetic isotope effect associated with acetyl-CoA carboxylation is –6.8
444 / 0.889 = –7.8‰ ($^{12}k/^{13}k = 1.0078$). Considering the isotope fractionation associated with ACC,
445 the difference between adjacent positions becomes –7.8‰, and the overall pattern becomes
446 consistent with the measurements of this study (Fig. 8). We note that $\Delta\delta^{13}C_{CH3\text{-}CH2a}$ is slightly
447 higher form sunflower than coconut (Fig. 5), a difference likely due to different fluxes or to

448 different kinetic isotope effect, or a combination of both. This difference might also be due to
449 the carbon chain length and their abundance in studied organisms (C18:1 and C16:0 are the
450 most abundant fatty acids in sunflower and coconut oil respectively). Furthermore, the
451 discussion above is based on differences between two adjacent positions, while it is clear from
452 Fig. 4 that between distant positions arising from the same positions of acetyl-CoA can show
453 large differences (e.g., positions C-2 and C-8 in C18:1 sunflower exhibit a 10‰ difference).
454 The calculation presented here is thus admittedly simplistic and awaits further data on the
455 position-specific isotope composition of natural compounds such as pyruvate and acetyl-CoA
456 as well as kinetic isotope effects of enzymes involved in fatty acids biosynthesis. Importantly,
457 the reaction catalyzed by ACC, while playing a role in determining the position-specific isotope
458 composition, will not influence the bulk isotope composition of fatty acids, simply because in
459 plastids, acetyl-CoA is fully committed to their biosynthesis (Alonso et al., 2007). Hence, the
460 ^{13}C-depletion on malonyl-CoA is compensated, by mass balance, by the ^{13}C-enrichment on the
461 acetyl-CoA, which must be true considering that fatty acids biosynthesis is at the steady state
462 (Alonso et al., 2010).

463 According to the fatty acids' elongation mechanism (Fig. 7), the isotopic fractionation
464 associated with the carboxylation of acetyl-CoA catalyzed by ACC is the main explanation for
465 the intramolecular ^{13}C distribution pattern within fatty acids (Chan and Vogel, 2010). However,
466 the relative ^{13}C depletion of fatty acids compared to other metabolites remains poorly explained.
467 Fatty acids elongation being carried out by consecutive addition of ^{13}C depleted malonyl-CoA,
468 a carbon-chain length effect could be expected; the longer fatty acids, the more ^{13}C depleted
469 carbons (from malonyl-CoA) they contain. However, simple calculation demonstrate that this
470 effect is negligible (see Fig. S1, supporting information) and other fractionation steps need to
471 be considered. The ^{13}C depletion of fatty acids compared to their sugar source was previously
472 explained by the "fragmentation-fractionation" phenomenon (Tcherkez et al., 2004) consisting
473 in the presence of a 1–2‰ isotopic fractionation associated with the cleavage of sugar to

474 produce pyruvate. As the conversion of pyruvate to acetyl-CoA is nearly quantitative in plant
475 seeds (no PDH associated fractionation), "fragmentation-fractionation" remains the best
476 explanation for the ^{13}C depletion of studied fatty acids. More isotopic fractionation sources
477 (dehydrogenation, transport, *de novo* synthesis, β-oxidation…) need to be considered when
478 studying more complex systems such as bacteria (e.g. *E. coli*), yeasts (e.g. *S. cerevisiae*) or
479 plant leaves.

480 *3.4 Implications*

481 The results presented here can be discussed considering previous data obtained in a series
482 of papers by Monson and Hayes through chemical degradation of fatty acids (1980, 1982a,
483 1982b) comparing their data summarized in Fig. 6 and those from the present study (Fig. 4).
484 Both Fig. 4 and 6 show the ^{13}C intramolecular isotope pattern within studied fatty acids, more
485 precisely the ^{13}C relative enrichment or depletion of each studied carbon-position. Fatty acids
486 isolated from *S. cerevisiae* grown on C_4 glucose qualitatively agrees with those obtained here,
487 with even positions depleted by 2.5‰ compared with the precursor, which could be explained
488 by an isotope effect associated with ACC. Nevertheless, the metabolic pathways in *S. cerevisiae*
489 are complex and involve transport in and out of the mitochondria as well as degradation of fatty
490 acids. Furthermore, another metabolic process needs to be considered when working with *S.*
491 *cerevisiae*: the Crabtree effect. When yeast such as *S. cerevisiae* are cultivated in aerobic
492 conditions using high concentrations of glucose (> 150 mg/L) a non-negligible amount of
493 glucose is converted into ethanol through fermentation (Verduyn et al., 1984). In presence of
494 high glucose concentration, the glycolysis is accelerated and a lot of ATP is generated which
495 lower the need of ATP production by TCA cycle. As a consequence, the oxygen consumption
496 is diminished resulting in the presence of glucose fermentation and the generation of ethanol
497 (De Deken, 1966; Barford and Hall, 1979; Postma et al., 1989). Monson and Hayes (1982) used
498 1.7 g/L glucose for their *S. cerevisiae* aerobic cultures which ensure the presence of a high

499 Crabtree effect during their yeast culture (Monson and Hayes, 1982b). In this context, measured
500 isotopic data may be altered while studying fatty acids biosynthesis.

501 Fatty acids from *E. coli* grown on a C_4 glucose as the sole carbon source displayed a 6‰
502 depletion on odd positions and negligible isotope fractionation on even positions. The data
503 agree well with the PDH reaction as the sole determinant in the bulk and position-specific
504 isotope composition of fatty acids. The results of Monson and Hayes (1980) reverse those
505 obtained here from vegetable oils. Several reasons can explain the discrepancy. First, as stated
506 above, the commitment of pyruvate to decarboxylation reaction is nearly quantitative in plant
507 plastids, making the isotope fractionation associated with PDH negligible. Second, the substrate
508 used by Monson and Hayes is C_4 glucose while C_3 plants studied here use sucrose as the main
509 transport carbohydrate. The expected relative ^{13}C-enrichment on the methyl and carbonyl
510 positions of pyruvate can be calculated based on recent measurements of sugars intramolecular
511 ^{13}C-pattern (Gilbert et al. 2012). For C_4 glucose the relative ^{13}C-enrichment is 0.4‰ and –1.3‰
512 for methyl and carbonyl positions, respectively, while it is –3.7‰ and –0.2‰ for C_3 sucrose.
513 Hence, considering only the starting sugar, the odd-even isotope fractionation should be
514 reversed. The absence of isotope fractionation in even positions seem in disagreement with the
515 data obtained in the present study which suggest a ^{13}C-depletion on the CH_2 position of
516 malonyl-CoA, and thus to a depletion on even positions (except the CH_3 position) of fatty acids.
517 The depletion should be much larger since the commitment of acetyl-CoA to fatty acids in *E.*
518 *coli* is only 20%, the other fates are acetate excretion (59%) citrate synthesis (14%), and
519 undetermined (6%) (Chen et al., 2011). The depletion on the CH_2 position of malonyl-CoA
520 must thus of the order of 6.2‰ (= 7.8 × (1 – 0.2); that is, assuming an isotope effect of 7.8‰)
521 which is at odds with the negligible value measured by Monson and Hayes (1980). Acetate
522 excretion is not likely to be associated with isotope fractionation on the CH_3 position of acetyl-
523 CoA since the latter is not involved in the reaction. However, citrate synthase reaction binds
524 the CH_3 position to the CO position of oxaloacetate. An isotope effect of 1.023 has been

suggested by Tcherkez and Farquhar (2005) based on the geometry and vibration frequencies of the transition state. Commitment to citrate synthase varies from 0.14 (Chen et al., 2011) to 0.29 (Schuetz et al., 2007), leading to a ^{13}C-enrichment on the CH_3 position of the remaining acetyl-CoA ranging from 3.2‰ to 6.7‰. This could therefore "compensate" for the ^{13}C-depletion associated with malonyl-CoA formation. This is also consistent with a negligible isotope fractionation on the methyl position (compared with the starting glucose) of excreted acetate as measured by Blair et al. (1985). The strong ^{13}C-enrichment on the COOH position of excreted acetate is more problematic and has not found any explanation yet. The fluxes of acetate re-assimilation seem to be controlled by the extracellular acetate concentration (Enjalbert et al., 2017). Therefore, measurements of intramolecular ^{13}C pattern of acetate and acetogenic lipids from *E. coli* grown in controlled conditions would be desirable.

Overall and considering all reactions leading to and consuming acetyl-CoA, our findings are consistent with that of Monson and Hayes (1980) but highlight the importance of reactions others than PDH as determinant of fatty acids bulk and intramolecular isotope composition. Interestingly, the patterns of fatty acids obtained here are consistent with measured on odd-numbered *n*-alkanes by (Gilbert et al., 2013), with the same relative enrichment on the terminal position compared to the next even position (Fig. 9). The exact origin of these n-alkanes is not known, but this result suggests that the ^{13}C intramolecular isotopic pattern observed within long-chain fatty acids could be preserved through diagenesis. Thereby, the PSIA of both fatty acids and *n*-alkanes can provide information on the biological origin of fossil hydrocarbons and potentially changes in metabolic pathways through geological time. The current NMR technique requires milligrams of pure fatty acids to perform PSIA, but the continuous development of this method lowers the required amount of analyte (Haddad et al., 2021). In addition, the use of high-resolution mass spectrometry such as the hybrid quadrupole-Orbitrap mass spectrometer has also proven a great capability to measure heavy isotope intramolecular distribution at micromole level (Neubauer et al., 2018). These technical advances represent the

551 future of PSIA for organic biogeochemistry making possible the analysis of samples from
552 sediments.

553 **4. Conclusions**

554 The data provided by the present study confirm the presence of a non-stochastic ^{13}C
555 intramolecular distribution within fatty acids, with the alternance of ^{13}C-enriched (odd) and ^{13}C-
556 depleted (even) carbon positions. This pattern and its amplitude are explained by the ^{13}C
557 distribution within acetyl-CoA directly inherited from fructose-6-phosphate (in C_3 plants) and
558 the isotope effect associated with the carboxylation of acetyl-CoA catalyzed by the acetyl-CoA
559 carboxylase (ACC) during fatty acids elongation. The isotopic fractionation associated with this
560 enzymatic reaction explains (i) the presence of relatively ^{13}C-enriched CH_3 compared to other
561 even carbon positions and (ii) the small increase of $\delta^{13}C$ difference between adjacent positions
562 compared to the $\Delta\delta^{13}C$ within acetyl-CoA. In addition, these data demonstrate that the ^{13}C
563 distribution within fatty acids and their relative ^{13}C depletion compared to the other metabolites
564 are not a consequence of PDH catalyzed conversion of pyruvate as this reaction is nearly
565 quantitative.

566 The ^{13}C intramolecular isotopic pattern within measured fatty acids and within long-chain
567 *n*-alkanes (Gilbert et al., 2013) are similar, suggesting the pattern can be inherited by *n*-alkanes
568 and as such be used as a biogeochemical indicator. Such data demonstrate the great interest of
569 fatty acids and, more generally, lipids PSIA to characterize the origin of organic matter found
570 in petroleum, sediments and rocks. The determination of ^{13}C intramolecular isotopic pattern
571 within both lipids from different organisms and fossil lipid hydrocarbons can be used to deduce
572 information on their origin(s) and history.

573

574

Acknowledgements

This work was financially supported by a grant-in-aid from Japan Society for the Promotion of Science (JSPS) n°17H06105 to NY, KM, AG, and MJ, as well as a grant-in-aid from Japan Society for the Promotion of Science (JSPS) n°18H01326 to AG. MJ also thanks the JSPS (n°P17725) for funding his postdoctoral fellowship. Financial support from the Chinese NSF [41973072 to YPZ, and 42007408 to RM] and China Postdoctoral Science Foundation [2019M650253 to RM] is gratefully acknowledged. This is the contribution #26 of the Isotopomics in Chemical Biology (ICB) group. The authors also acknowledge the anonymous reviewers and the Associate Editor for their constructive comments.

References

Akoka, S., Remaud, G.S., 2020. NMR-based isotopic and isotopomic analysis. Progress in nuclear magnetic resonance spectroscopy 120–121, 1–24.

Alonso, A.P., Goffman, F.D., Ohlrogge, J.B., Shachar-Hill, Y., 2007. Carbon conversion efficiency and central metabolic fluxes in developing sunflower (*Helianthus annuus L.*) embryos. The Plant Journal 52, 296–308.

Barford, J.P., Hall, R.J., 1979. An examination of the Crabtree effect in *Saccharomyces cerevisiae*: the role of respiratory adaptation. Microbiology 114, 267–275.

Bayle, K., Gilbert, A., Julien, M., Yamada, K., Silvestre, V., Robins, R.J., Akoka, S., Yoshida, N., Remaud, G.S., 2014. Conditions to obtain precise and true measurements of the intramolecular ^{13}C distribution in organic molecules by isotopic ^{13}C nuclear magnetic resonance spectrometry. Analytica Chimica Acta 846, 1–7.

599 Bayle, K., Grand, M., Chaintreau, A., Robins, R.J., Fieber, W., Sommer, H., Akoka, S.,
600 Remaud, G.S., 2015. Internal referencing for ^{13}C position-specific isotope analysis
601 measured by NMR spectrometry. Analytical Chemistry.
602 doi:10.1021/acs.analchem.5b02094
603 Billault, I., Guiet, S., Mabon, F., Robins, R., 2001. Natural deuterium distribution in long-chain
604 fatty acids is nonstatistical: a site-specific study by quantitative ^{2}H NMR spectroscopy.
605 ChemBioChem 2, 425–431.
606 Blair, N., Leu, A., Muñoz, E., Olsen, J., Kwong, E., Des Marais, D., 1985. Carbon isotopic
607 fractionation in heterotrophic microbial metabolism. Applied and Environmental
608 Microbiology 50, 996–1001.
609 Botosoa, E.P., Caytan, E., Silvestre, V., Robins, R.J., Akoka, S., Remaud, G.S., 2008.
610 Unexpected fractionation in site-specific ^{13}C isotopic distribution detected by
611 quantitative ^{13}C NMR at natural abundance. Journal of the American Chemical Society
612 130, 414–415.
613 Caytan, E., Botosoa, E.P., Silvestre, V., Robins, R.J., Akoka, S., Remaud, G.S., 2007. Accurate
614 quantitative ^{13}C NMR spectroscopy: repeatability over time of site-specific ^{13}C isotope
615 ratio determination. Analytical Chemistry 79, 8266–8269.
616 Chan, D.I., Vogel, H.J., 2010. Current understanding of fatty acid biosynthesis and the acyl
617 carrier protein. Biochemical Journal 430, 1–19.
618 Chapman, G.W., 1979. Gas chromatographic determination of free fatty acids in vegetable oils
619 by a modified esterification procedure. Journal of the American Oil Chemists' Society
620 56, 77–79.
621 Chawla, B., 2003. An automated transesterification technique for quantitation of acid
622 precursors of ester-based oils. Journal of Chromatographic Science 41, 560–563.

Chen, X., Alonso, A.P., Allen, D.K., Reed, J.L., Shachar-Hill, Y., 2011. Synergy between ^{13}C-metabolic flux analysis and flux balance analysis for understanding metabolic adaption to anaerobiosis in *E. coli.* Metabolic Engineering 13, 38–48.

Chimiak, L., Elsila, J.E., Dallas, B., Dworkin, J.P., Aponte, J.C., Sessions, A.L., Eiler, J.M., 2021. Carbon isotope evidence for the substrates and mechanisms of prebiotic synthesis in the early solar system. Geochimica et Cosmochimica Acta 292, 188–202.

Corso, T.N., Brenna, J.T., 1997. High-precision position-specific isotope analysis. Proceedings of the National Academy of Sciences 94, 1049–1053.

De Deken, R.H., 1966. The Crabtree Effect: A regulatory system in yeast. Microbiology 44, 149–156.

DeNiro, M.J., Epstein, S., 1977. Mechanism of carbon isotope fractionation associated with lipid synthesis. Science 197, 261–263.

Diomande, D.G., Martineau, E., Gilbert, A., Nun, P., Murata, A., Yamada, K., Watanabe, N., Tea, I., Robins, R.J., Yoshida, N., Remaud, G.S., 2015. Position-specific isotope analysis of xanthines: a ^{13}C nuclear magnetic resonance method to determine the ^{13}C intramolecular composition at natural abundance. Analytical Chemistry 87, 6600–6606.

Duan, J.-R., Billault, I., Mabon, F., Robins, R., 2002. Natural deuterium distribution in fatty acids isolated from peanut seed oil: a site-specific study by quantitative ^{2}H NMR spectroscopy. ChemBioChem 3, 752–759.

Duron, O.S., Nowotny, Alois., 1963. Microdetermination of long-chain carboxylic acids by transesterification with boron trifluoride. Analytical Chemistry 35, 370–372.

Eiler, J.M., Clog, M., Magyar, P., Piasecki, A., Sessions, A., Stolper, D., Deerberg, M., Schlueter, H.-J., Schwieters, J., 2013. A high-resolution gas-source isotope ratio mass spectrometer. International Journal of Mass Spectrometry 335, 45–56.

Enjalbert, B., Millard, P., Dinclaux, M., Portais, J.-C., Létisse, F., 2017. Acetate fluxes in *Escherichia coli* are determined by the thermodynamic control of the Pta-AckA pathway. Scientific Reports 7, 42135.

Gilbert, A., Silvestre, V., Robins, R.J., Remaud, G.S., 2009. Accurate quantitative isotopic ^{13}C NMR spectroscopy for the determination of the intramolecular distribution of ^{13}C in glucose at natural abundance. Analytical Chemistry 81, 8978–8995.

Gilbert, A., Silvestre, V., Robins, R.J., Tcherkez, G., Remaud, G.S., 2011. A ^{13}C NMR spectrometric method for the determination of intramolecular $\delta^{13}C$ values in fructose from plant sucrose samples. New Phytologist 191, 579–588.

Gilbert, A., Silvestre, V., Robins, R.J., Remaud, G.S., Tcherkez, G., 2012. Biochemical and physiological determinants of intramolecular isotope patterns in sucrose from C_3, C_4 and CAM plants accessed by isotopic ^{13}C NMR spectrometry: a viewpoint. Natural Product Reports 29, 476–486.

Gilbert, A., Robins, R.J., Remaud, G.S., Tcherkez, G.G., 2012. Intramolecular ^{13}C pattern in hexoses from autotrophic and heterotrophic C_3 plant tissues. Proceedings of the National Academy of Sciences of the United States of America 109, 18204–9.

Gilbert, A., Yamada, K., Yoshida, N., 2013. Exploration of intramolecular ^{13}C isotope distribution in long chain *n*-alkanes (C_{11}–C_{31}) using isotopic ^{13}C NMR. Organic Geochemistry 62, 56–61.

Gilbert, A., Yamada, K., Suda, K., Ueno, Y., Yoshida, N., 2016. Measurement of position-specific ^{13}C isotopic composition of propane at the nanomole level. Geochimica et Cosmochimica Acta 177, 205–216.

Gilbert, A., 2021. The organic isotopologue frontier. Annual Review of Earth and Planetary Sciences 49, 435–464.

Haddad, L., Renou, S., Remaud, G.S., Rizk, T., Bejjani, J., Akoka, S., 2021. A precise and rapid isotopomic analysis of small quantities of cholesterol at natural abundance by optimized

^{1}H-^{13}C 2D NMR. Analytical and Bioanalytical Chemistry 413, 1521–1532.

Hayes, J.M., 1993. Factors controlling ^{13}C contents of sedimentary organic compounds: principles and evidence. Marine Geology 113, 111–125.

Hayes, J.M., 2001. Fractionation of carbon and hydrogen isotopes in biosynthetic processes. Reviews in Mineralogy and Geochemistry 43, 225–277.

Jézéquel, T., Joubert, V., Giraudeau, P., Remaud, G.S., Akoka, S., 2017. The new face of isotopic NMR at natural abundance. Magnetic Resonance in Chemistry 55, 77–90.

Julien, M., Nun, P., Höhener, P., Parinet, J., Robins, R.J., Remaud, G.S., 2016. Enhanced forensic discrimination of pollutants by position-specific isotope analysis using isotope ratio monitoring by ^{13}C nuclear magnetic resonance spectrometry. Talanta 147, 383–389.

Julien, M., Liégeois, M., Höhener, P., Paneth, P., Remaud, G.S., 2021. Intramolecular non-covalent isotope effects at natural abundance associated with the migration of paracetamol in solid matrices during liquid chromatography. Journal of Chromatography A 1639, 461932.

Lesot, P., Berdagué, P., Silvestre, V., Remaud, G., 2021. Exploring the enantiomeric ^{13}C position-specific isotope fractionation: challenges and anisotropic NMR-based analytical strategy. Analytical and Bioanalytical Chemistry 413 (25), 6379-6392.

Melzer, E., Schmidt, H.L., 1987. Carbon isotope effects on the pyruvate dehydrogenase reaction and their importance for relative carbon-13 depletion in lipids. The Journal of Biological Chemistry 262, 8159–8164.

Metcalfe, L.D., Schmitz, A.A., Pelka, J.R., 1966. Rapid preparation of fatty acid esters from lipids for gas chromatographic analysis. Analytical Chemistry 38, 514–515.

Monson, K.D., Hayes, J.M., 1980. Biosynthetic control of the natural abundance of carbon-13 at specific positions within fatty acids in *Escherichia coli*. Evidence regarding the

coupling of fatty acid and phospholipid synthesis. Journal of Biological Chemistry 255, 11435–11441.

Monson, K.D., Hayes, J.M., 1982a. Carbon isotopic fractionation in the biosynthesis of bacterial fatty acids. Ozonolysis of unsaturated fatty acids as a means of determining the intramolecular distribution of carbon isotopes. Geochimica et Cosmochimica Acta 46, 139–149.

Monson, K.D., Hayes, J.M., 1982b. Biosynthetic control of the natural abundance of carbon-13 at specific positions within fatty acids in *Saccharomyces cerevisiae*. Isotopic fractionation in lipid synthesis as evidence for peroxisomal regulation. Journal of Biological Chemistry 257, 5568–5575.

Morrison, W.R., Smith, L.M., 1964. Preparation of fatty acid methyl esters and dimethylacetals from lipids with boron fluoride-methanol. Journal of lipid research 5, 600–608.

Neubauer, C., Sweredoski, M.J., Moradian, A., Newman, D.K., Robins, R.J., Eiler, J.M., 2018. Scanning the isotopic structure of molecules by tandem mass spectrometry. International Journal of Mass Spectrometry 434, 276–286.

Alonso, A., Dale, V.L., Shachar-Hill, Y., 2010. Understanding fatty acid synthesis in developing maize embryos using metabolic flux analysis. Metabolic Engineering 12, 488–497.

Portaluri, V., Thomas, F., Jamin, E., Lorandel, B., Silvestre, V., Akoka, S., Remaud, G.S., 2021. Vanillin isotopic intramolecular ^{13}C profile through polarization transfer NMR pulse sequence and statistical modelling. Food Control 130, 108345.

Postma, E., Verduyn, C., Scheffers, W.A., Van Dijken, J.P., 1989. Enzymic analysis of the crabtree effect in glucose-limited chemostat cultures of *Saccharomyces cerevisiae*. Applied and Environmental Microbiology 55, 468–477.

Roberts, R.B., Cowie, D.B., Abelson, P.H., Bolton, E.T., Britten, R.J., 1955. Studies of biosynthesis of *Escherichia coli*. The Quarterly Review of Biology 31, 155–156.

Rossmann, A., Butzenlechner, M., Schmidt, H.-L., 1991. Evidence for a nonstatistical carbon isotope distribution in natural glucose. Plant physiology 96, 609–614.

Schouten, S., Klein Breteler, W.C.M., Blokker, P., Schogt, N., Rijpstra, W.I.C., Grice, K., Baas, M., Sinninghe Damsté, J.S., 1998. Biosynthetic effects on the stable carbon isotopic compositions of algal lipids: implications for deciphering the carbon isotopic biomarker record. Geochimica et Cosmochimica Acta 62, 1397–1406.

Schuetz, R., Kuepfer, L., Sauer, U., 2007. Systematic evaluation of objective functions for predicting intracellular fluxes in *Escherichia coli*. Molecular Systems Biology 3, 119.

Schwender, J., Shachar-Hill, Y., Ohlrogge, J.B., 2006. Mitochondrial metabolism in developing embryos of *Brassica napus*. Journal of Biological Chemistry 281, 34040–34047.

Silvestre, V., Mboula, V.M., Jouitteau, C., Akoka, S., Robins, R.J., Remaud, G.S., 2009. Isotopic ^{13}C NMR spectrometry to assess counterfeiting of active pharmaceutical ingredients: site-specific ^{13}C content of aspirin and paracetamol. Journal of Pharmaceutical and Biomedical Analysis 50, 336–341.

Tcherkez, G., Farquhar, G., Badeck, F., Ghashghaie, J., 2004. Theoretical considerations about carbon isotope distribution in glucose of C_3 plants. Functional Plant Biology 31, 857–877.

Tcherkez, G., Farquhar, G.D., 2005. Carbon isotope effect predictions for enzymes involved in the primary carbon metabolism of plant leaves. Functional Plant Biology 32, 277–291.

Tenailleau, E., Remaud, G., Akoka, S., 2005. Quantification of the ^{1}H-decoupling effects on the accuracy of ^{13}C-NMR measurements. Instrumentation Science & Technology 33, 391–399.

Tenailleau, E., Akoka, S., 2007. Adiabatic ^{1}H decoupling scheme for very accurate intensity measurements in ^{13}C NMR. Journal of Magnetic Resonance 185, 50–8.

Thomas, F., Randet, C., Gilbert, A., Silvestre, V., Jamin, E., Akoka, S., Remaud, G., Segebarth, N., Guillou, C., 2010. Improved characterization of the botanical origin of sugar by

carbon-13 SNIF-NMR applied to ethanol. Journal of agricultural and food chemistry 58, 11580–5.

Valentine, D.L., 2009. Isotopic remembrance of metabolism past. Proceedings of the National Academy of Sciences 106, 12565–12566.

van der Meer, M.T.J., Schouten, S., Sinninghe Damsté, J.S., 1998. The effect of the reversed tricarboxylic acid cycle on the ^{13}C contents of bacterial lipids. Organic Geochemistry 28, 527–533.

Verduyn, C., Zomerdijk, T.P.L., van Dijken, J.P., Scheffers, W.A., 1984. Continuous measurement of ethanol production by aerobic yeast suspensions with an enzyme electrode. Applied Microbiology and Biotechnology 19, 181–185.

Vogler, E.A., Hayes, J.M., 1979. Carbon isotopic fractionation in the Schmidt decarboxylation: evidence for two pathways to products. The Journal of Organic Chemistry 44, 3682–3686.

Volchkov, I., Park, S., Lee, D., 2011. Ring strain-promoted allylic transposition of cyclic silyl ethers. Organic Letters 13, 3530–3533.

Yamada, K., Kikuchi, M., Gilbert, A., Yoshida, N., Wasano, N., Hattori, R., Hirano, S., 2014. Evaluation of commercially available reagents as a reference material for intramolecular carbon isotopic measurements of acetic acid. Rapid Communication in Mass Spectrometry 28, 1821–1828.

Zhou, Y., Grice, K., Stuart-Williams, H., Farquhar, G.D., Hocart, C.H., Lu, H., Liu, W., 2010. Biosynthetic origin of the saw-toothed profile in $\delta^{13}C$ and $\delta^{2}H$ of *n*-alkanes and systematic isotopic differences between *n*-, *iso*- and *anteiso*-alkanes in leaf waxes of land plants. Phytochemistry 71, 388–403.

Appendix A. Supplementary information

Figure captions

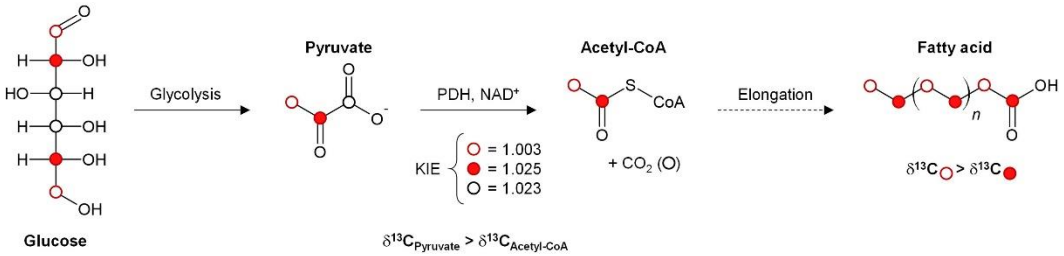

Fig. 1: Conventional view of the origin of the ^{13}C-depletion of acetogenic lipids. The pyruvate dehydrogenase (PDH) reaction is associated with a kinetic isotope effect leading to a ^{13}C-depletion on the CO position of acetyl-CoA, and thus on all odd positions of fatty acids. Fatty acids thus have a "zig-zag" isotope pattern where odd positions are ^{13}C-depleted compared to even ones. Position-specific isotope effects (^{12}k/^{13}k) are indicated with the color corresponding to the C-atom of the starting pyruvate, according to DeNiro and Epstein 1977.

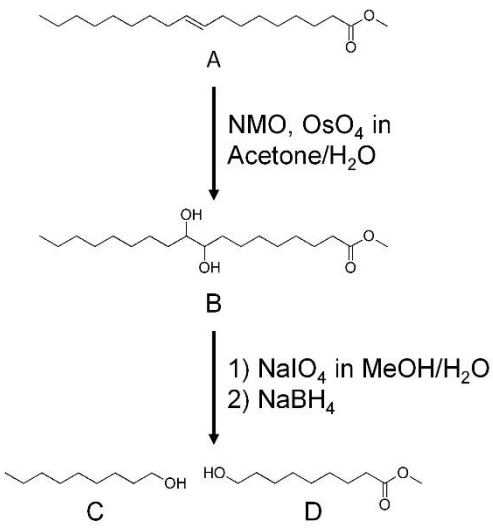

Fig. 2: Chemical cleavage of methyl oleate (C18:1). Adapted from Billault *et al.* 2001.

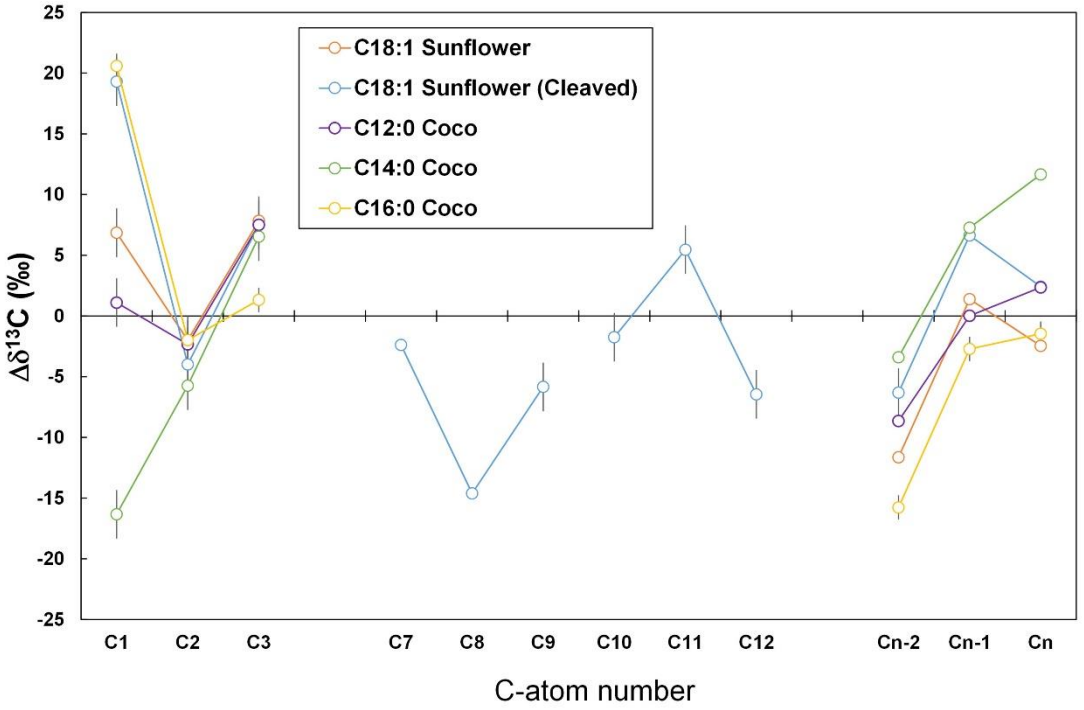

Fig. 3: $\Delta\delta^{13}C$ values of fatty acid methyl esters from coconut oil and sunflower oil. Carbon positions 9 and 10 are not connected here as they were measured through two different measurements.

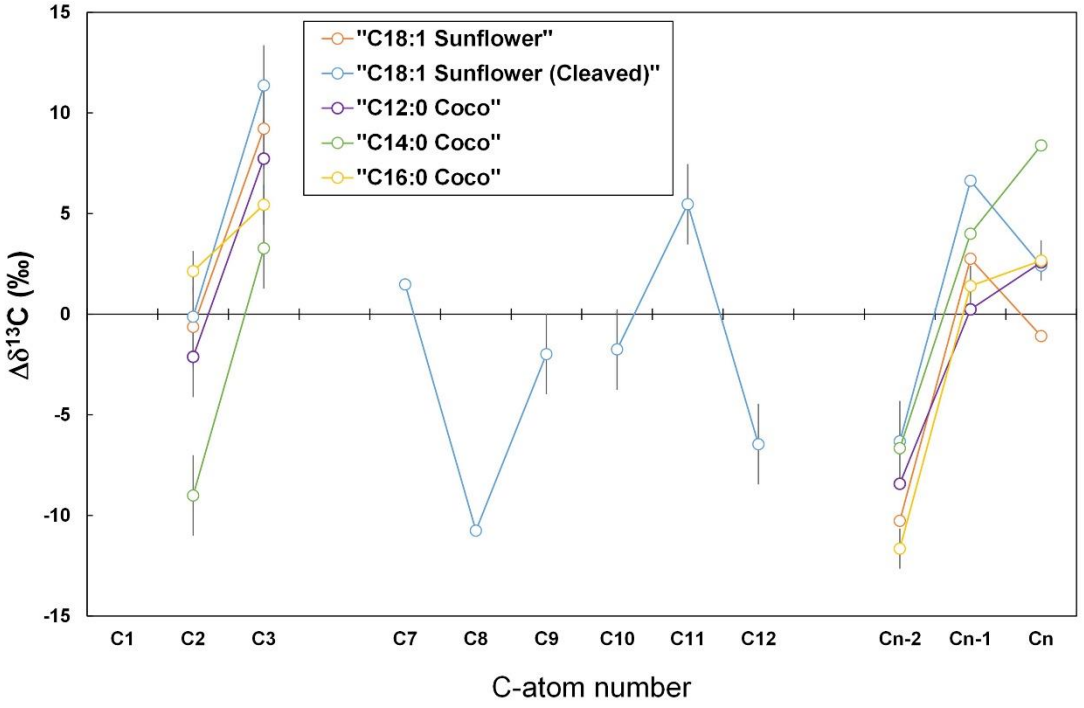

795

796 Fig. 4: $\Delta\delta^{13}C$ values of fatty acid methyl esters from coconut oil and sunflower oil. The values
797 have been calculated omitting the carboxyl position. Carbon positions 9 and 10 are not
798 connected here as they were measured through two different measurements.

799

800

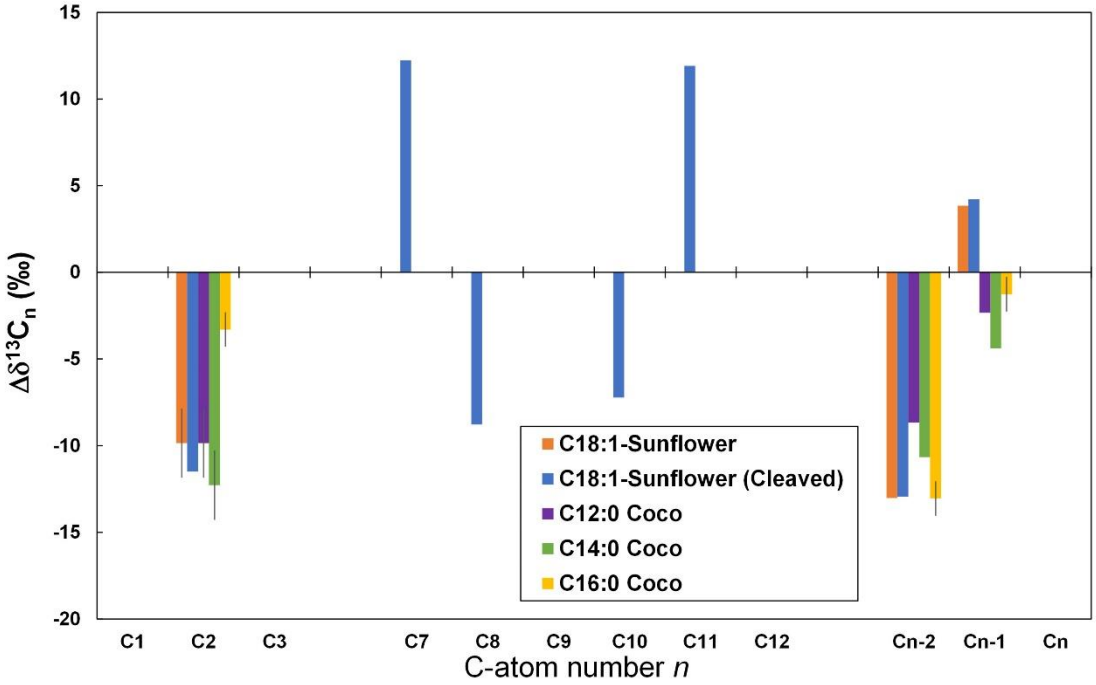

801

802 Fig. 5: Isotope fractionation between adjacent positions ($\Delta\delta^{13}C_n = \delta^{13}C_n - \delta^{13}C_{n+1}$) for fatty acid

803 methyl esters from coconut oil and sunflower oil.

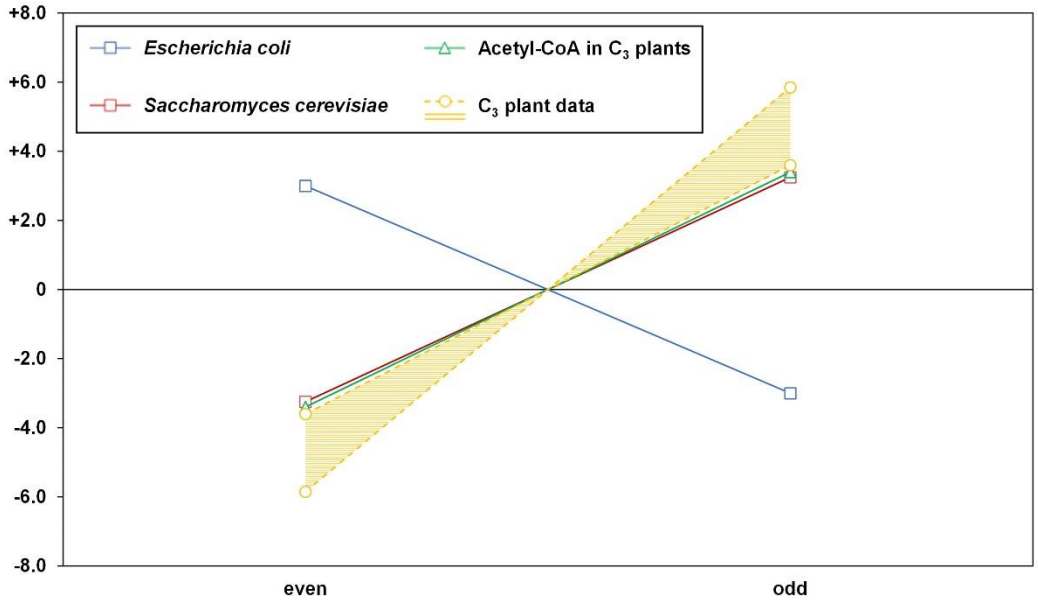

804

805 Fig. 6: Relative ^{13}C enrichment (in ‰) of even and odd carbon-positions of fatty acids from

806 *Escherichia coli* (Monson and Hayes 1980), *Saccharomyces cerevisiae* (Monson and Hayes

807 1982) and C_3 plants (coconut and sunflower) measured in this study. Also shown, the theoretical

808 ^{13}C distribution within acetyl-CoA in C_3 plants.

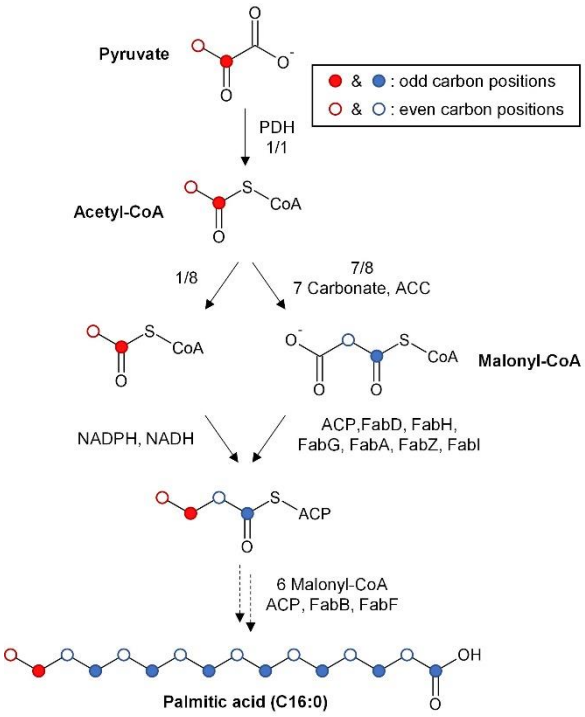

Fig. 7: Summarized fatty acid biosynthesis pathway describing the origin of carbon atoms, adapted from Chan and Vogel 2010. PDH: Pyruvate dehydrogenase, ACP: Acyl carrier protein, FabD: Malonyl-CoA–ACP transacylase, FabH: β-Oxoacyl synthase III, FabG: β-Oxoacyl reductase, FabA: β-Hydroxydecanoyl dehydratase , FabZ: β-Hydroxyacyl dehydratase, FabI: Enoyl reductase, FabB: β-Oxoacyl synthase I, FabF: β-Oxoacyl synthase II.

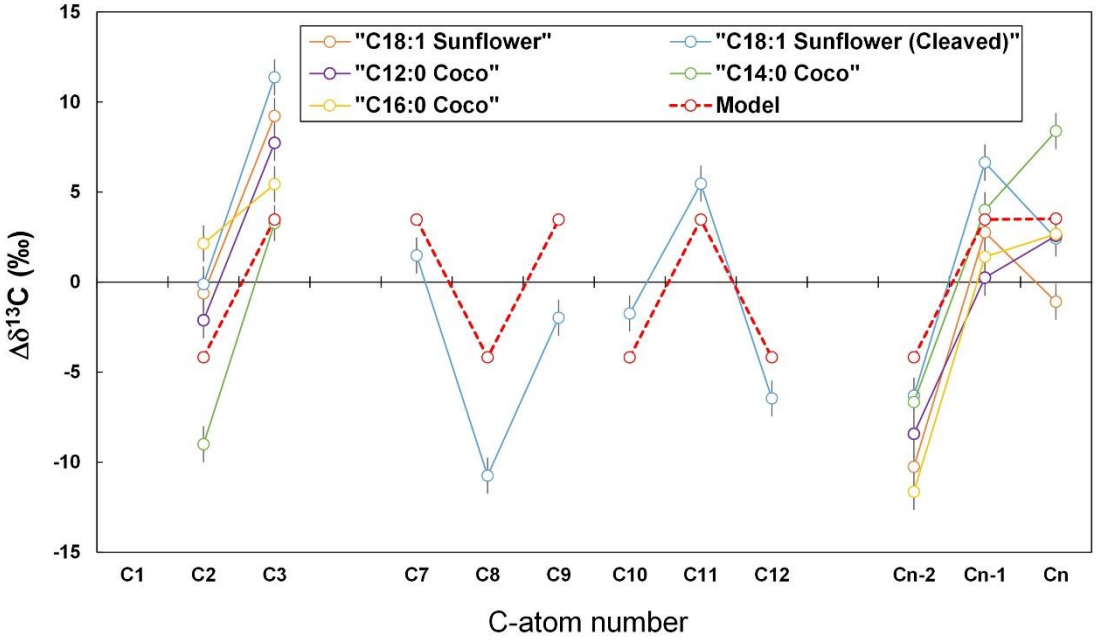

816

817 Fig. 8: Comparison of measurements of fatty acid methyl esters and a model implying an
818 isotope effect of 7.8‰ associated with acetyl-CoA carboxylation catalyzed by acetyl-CoA
819 carboxylase (ACC).

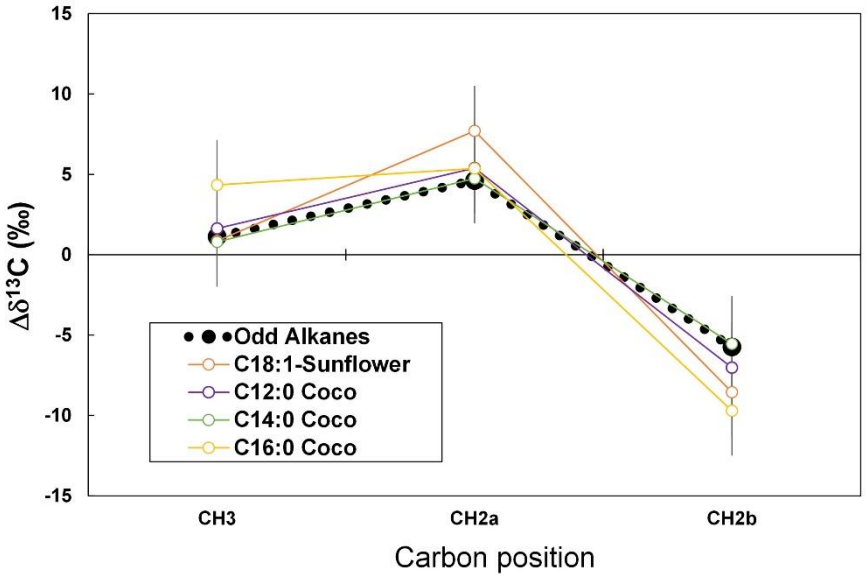

820

821 Fig. 9: Expected pattern of *n*-alkanes arising from the decarboxylation of the fatty acids
822 measured in this study. "Odd alkanes" is the average of the data for odd *n*-alkanes (C_{21}-C_{31})
823 measured by NMR (Gilbert et al. 2013).

Tables

Table 1: Bulk isotopic composition ($\delta^{13}C_{Bulk}$) and isotopic differences between adjacent positions for fatty acid methyl esters from coconut oil and sunflower oil (in ‰).

	Sunflower		Coconut			Average	sd
	C18:1	cleaved C18:1	C12:0	C14:0	C16:0		
$\delta^{13}C_{Bulk}$	–30.9	-	–29.4	–29.2	–30.1	-	-
$\delta^{13}C_{C2-C3}$	–9.9	–11.5	–9.8	–12.3	–3.3	–9.4	3.5
$\delta^{13}C_{C7-C8}$	-	+12.2	-	-	-	+12.2	-
$\delta^{13}C_{C8-C9}$	-	–8.8	-	-	-	–8.8	-
$\delta^{13}C_{C10-C11}$	-	–7.2	-	-	-	–7.2	-
$\delta^{13}C_{C11-C12}$	-	+11.9	-	-	-	+11.9	-
$\delta^{13}C_{C(n-2)-C(n-1)}$	–13.0	–12.9	–8.7	–10.7	–13.0	–11.7	2.0
$\delta^{13}C_{C(n-1)-Cn}$	+3.8	+3.9	–2.3	–4.4	–1.3	0.0	3.8